AD-759 506

STRUCTURAL PROPERTIES OF DUAL HARDNESS STEEL ARMOR

Albert A. Anctil, et al

Army Materials and Mechanics Research Center
Watertown, Massachusetts

February 1973

AMMRC TR 73-6

AD

STRUCTURAL PROPERTIES OF DUAL HARDNESS STEEL ARMOR

ALBERT A. ANCTIL, RICHARD CHAIT,
CHARLES H. CURLL, and ERIC B. KULA
METALS RESEARCH DIVISION

February 1973

Approved for public release; distribution unlimited.

ARMY MATERIALS AND MECHANICS RESEARCH CENTER
Watertown, Massachusetts 02172

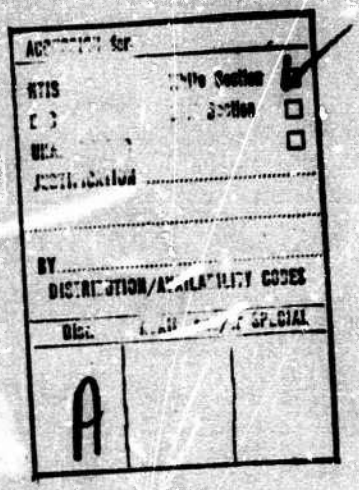

The findings in this report are not to be construed as an official Department of the Army position, unless so designated by other authorized documents.

Mention of any trade names or manufacturers in this report shall not be construed as advertising nor as an official indorsement or approval of such products or companies by the United States Government.

DISPOSITION INSTRUCTIONS

Destroy this report when it is no longer needed.
Do not return it to the originator.

AMMRC TR 73-6

STRUCTURAL PROPERTIES OF DUAL HARDNESS STEEL ARMOR

Technical Report by
ALBERT A. ANCTIL, RICHARD CHAIT, CHARLES H. CURLL, and ERIC B. KULA

February 1973

D/A Projects 1T062105A328 & 1F162205AA5201
AMCMS Codes 502E.11.294 & 512E.11.A52
Fatigue Crack Propagation of High Strength Steels
Agency Accession Numbers DA OC4815 & OC4808

METALS RESEARCH DIVISION
ARMY MATERIALS AND MECHANICS RESEARCH CENTER
Watertown, Massachusetts 02172

AMMRC Ex. O's. 32162 & 32262

UNCLASSIFIED
Security Classification

DOCUMENT CONTROL DATA - R & D

(Security classification of title, body of abstract and indexing annotation must be entered when the overall report is classified)

1. ORIGINATING ACTIVITY (Corporate author)
Army Materials and Mechanics Research Center
Watertown, Massachusetts 02172

2a. REPORT SECURITY CLASSIFICATION
Unclassified

2b. GROUP

3. REPORT TITLE
STRUCTURAL PROPERTIES OF DUAL HARDNESS STEEL ARMOR

4. DESCRIPTIVE NOTES (Type of report and inclusive dates)

5. AUTHOR(S) (First name, middle initial, last name)
Albert A. Anctil, Richard Chait, Charles H. Curli, and Eric B. Kula

6. REPORT DATE	7a. TOTAL NO. OF PAGES	7b. NO. OF REFS
February 1973	~~22~~ 24	9

8a. CONTRACT OR GRANT NO.

b. PROJECT NO. D/A 1T026105A328 & D/A 1F162205AA5201

c. AMCMS Code 502E.11.294 & 512E.11.A52

d. Agency Accession No. DA OC4815 & OC4808

9a. ORIGINATOR'S REPORT NUMBER(S)
AMMRC TR 73-6

9b. OTHER REPORT NO(S) (Any other numbers that may be assigned this report)

10. DISTRIBUTION STATEMENT
Approved for public release; distribution unlimited.

11. SUPPLEMENTARY NOTES
Funding appropriated under two Department of the Army projects identified in block 8.

12. SPONSORING MILITARY ACTIVITY
U. S. Army Materiel Command
Washington, D. C. 20315

13. ABSTRACT

Because of interest in the Aerial Reconnaissance System there has been increased emphasis on the load-carrying capabilities of dual hardness steel (DHS) armor material. This material is a composite consisting of a high-hardness, high-carbon frontal plate metallurgically bonded to a softer lower carbon steel backup. Since the concept of DHS used for both structural and armor purposes is new, relatively little information is available to designers on the structural properties after ballistic impact. In the present paper, four different lots of DHS having target hardness levels of R_c 60 for the frontal portion and R_c 50 for the backup are considered. One lot was produced by standard ausforming techniques while the other three were conventionally produced heat-treatable roll-bonded steels. Base-line mechanical property data are given. These include tensile, fatigue crack propagation, and S-N behavior. The effects of varying temperature and frequency on crack propagation rate are shown. Ballistically damaged specimens are utilized to provide information on residual strength and residual life. (Authors)

DD FORM 1 NOV 68 1473 REPLACES DD FORM 1473, 1 JAN 68, WHICH IS OBSOLETE FOR ARMY USE.

UNCLASSIFIED
Security Classification

14 KEY WORDS	LINK A		LINK B		LINK C	
	ROLE	WT	ROLE	WT	ROLE	WT
Steels - armor						
Composite armor						
Ballistic damage						
Aircraft armor						
Fractures (materials)						
Fracture properties						

U.S. GOVERNMENT PRINTING OFFICE: 1973 701-783/116

CONTENTS

INTRODUCTION

Recent concepts of improved helicopter protection against small arms fire utilize steel armor that provides both load-carrying and ballistic protection capability. Such an approach may be the backbone of the Aerial Armored Reconnaissance System (AARS). For such an application, a leading candidate material is a dual hardness steel (DHS) composite consisting of a high-hardness, high-carbon frontal plate metallurgically bonded to a softer lower carbon steel backup portion. To date there has been considerable emphasis on the ballistic performance of DHS with some effort devoted to fabrication, notably cutting, forming, and finishing.[1,2] Although the concept of DHS is relatively old, its use as a structural armor material is relatively new, and hence little information is available for the designer. This material poses interesting problems to the designer since the frontal material with its hardness of R_c 60 is considerably harder and stronger but less tough than more common high strength structural steels, and also because DHS is a layered composite with overall properties dependent on the size and properties of the individual components as well as the integrity of the interfacial bond. Furthermore, since the material is constantly being improved, important properties have not been completely standardized nor characterized. Recent efforts at the Army Materials and Mechanics Research Center have focused on this problem.[3-6] It is the intent of the present paper to improve the understanding of DHS by providing some pertinent information from on-going studies that will shed some light on base-line mechanical properties, ballistic damage characterization, and ballistic damage effects on residual strength and life of several heats of DHS.

MATERIALS AND PROCEDURE

Materials

Four separate lots of DHS have been evaluated, one of which consisted of ausformed steels and the other three which were heat-treatable composites produced by roll bonding. Two of the latter were air melts, designated Lot I and Lot II, while the third was a vacuum induction melt, designated VIM. Nominal compositions and processing history are listed in Table I. All materials investigated were approximately 50% frontal material and 50% backup material.

Table I. SUMMARY OF DUAL HARDNESS STEELS

		Heat-Treatable Steel		
	Ausformed Steel	Air Melt Lot I	Air Melt Lot II	Vacuum Induction Melt
Composition Frontal Backup	0.41C-5Cr-1.3Mo-0.4V 0.31C-7.5Ni-1Cr-1Mo-4.3Co	0.57C-1Ni-0.8Cr-0.5Mo 0.31C-1Ni-0.8Cr-0.5Mo	0.62C-3.3Ni-0.4Mo 0.28C-3.3Ni-0.4Mo	0.54C-1Ni-0.75Cr-0.5Mo 0.31C-1Ni-0.75Cr-0.5Mo
Processing	Roll bond at 1900 F Quench to 1500 F, roll 54% Quench Temper at 400 F	Roll bond at 2275 F Oil Quench 1500 F Double temper at 250 F	Roll bond at 2275 F Oil Quench from 1500 F Double temper at 250 F	Roll bond at 2100 F Oil Quench from 1500 F Temper at 275 F
Plate Thickness	0.20 in.	0.22 in.	0.22 in.	0.22 in.

The ausformed steels, which are thermomechanically treated, develop their strength by extensively deforming the steel in the austenitic condition and directly quenching to form martensite. Therefore, any large amounts of forming must be done as part of the original processing, since these steels are generally supplied in the hard, heat-treated condition. The heat-treatable steel can be supplied in the annealed condition and then fabricated to shape and heat treated by the fabricator.

The interfacial bond between the frontal and backup materials is generally better in the heat-treatable DHS, since the higher roll bonding temperatures and greater time at temperature allow for greater interdiffusion between the two layers.

Mechanical Properties

Base-line mechanical properties including hardness, tension, fatigue, and crack growth were determined. Rockwell C hardness was measured on the front and rear surface of each plate. In some cases tensile properties were supplied by the producer. In two cases, the ausformed steel and air melt Lot I, properties were supplied on the backup and frontal material separately. These were determined from separate plates that had received the same processing and heat treatment as the composite DHS, rather than from specimens that were machined from the actual armor. For the three heat-treatable steels, tension tests were conducted on specimens machined from the composite armor, which included both the frontal and backup material. Standard half-inch-wide, two-inch gage length flat tension specimens were used.

In order to get an indication of the fatigue behavior of DHS, specimens similar to the flat tension specimens were machined from the air melt Lot II. These were tested in tension-tension fatigue at a minimum:maximum stress ratio of 0.1. The number of cycles to failure were determined as a function of maximum stress. These tests were generally conducted on specimens with an as-received surface, which may be typical of some applications.

Fatigue crack propagation data were obtained from center-notched specimens 3.0 inches wide and 12.0 inches long. Approximately 0.020 inch was ground off each surface. The center notch was electric-discharge machined perpendicular to the plate rolling direction. The specimens were subjected to sinusoidal loading with a constant mean load at 4 and 15 Hz with an axial-fatigue, hydraulic, closed-loop testing machine. The specimens are identified by the applied maximum gross section stress. The minimum gross section stress in all cases was 3.0 ksi. Crack growth was measured on the frontal and backup material simultaneously from the specimen center line to one edge. Measurements were made using a traveling microscope with 30 times magnification and stroboscopic illumination. The crack growth curves include the number of cycles necessary to initiate the fatigue crack from the 0.002-inch radius machined notch. Testing temperatures below room temperature were obtained by varying the flow of gas from a liquid nitrogen reservoir through a Plexiglas cell. The variation in temperature was ± 3 F.

Ballistic Damage

All ballistic tests were performed at the Army Materials and Mechanics Research Center ballistic test facility using caliber 0.30 ball M2 and armor piercing (AP) M2 projectiles. Ballistic performance (V_{50}) data were obtained but will not be discussed in the present paper. However, the relative damage resulting from ballistic impacts at several velocities will be discussed and categorized. Ballistic damage was assessed qualitatively by visual examination. In one series, Magnaflux testing was used to quantitatively measure the extent of cracking.

In one group of tests the applied stress during ballistic testing was introduced as a variable. A given projectile velocity was selected that would provide complete penetration. During ballistic testing a tensile load was applied to the 14-inch-long by 6-inch-wide specimen by hydraulic means. These specimens were used to determine the effect of the applied stress on the extent of ballistic damage. Limited tension testing was carried out on this group to determine the effect of steady stress during ballistic testing on residual strength.

Residual life fatigue data of ballistically damaged armor were obtained from specimens having the same dimensions as the crack growth specimens, three by twelve inches. These specimens were cut from armor plate that had been used to obtain a five-shot ballistic limit. Sinusoidal fatigue loading was used at 15 Hz between 3 to 10.5 or 3 to 18 ksi. During testing frequent photographs were taken of both surfaces to study the course of crack growth.

RESULTS AND DISCUSSION

Base-Line Mechanical Properties

The base-line mechanical properties for the various lots of DHS are listed in Table II. The target hardness was R_c 60 for the frontal material in order to provide resistance to ballistic penetration. For the backup material, a target hardness of R_c 50 was suggested. The two air melt lots came close to these values, while the hardness of the backup material for the VIM steel was slightly lower, R_c 48.

The tensile properties reported for the frontal and backup materials of the ausformed and air melt Lot I were determined on material processed separately, but in the same manner as the composite. The tensile strengths, 350 to 360 ksi for the frontal material, are extremely high for a structural material, but consistent with the high hardness.

For the air melt Lot II and the VIM steels, tensile properties were determined only on a composite specimen cut from the armor plate. For air melt Lot I a composite specimen was tested in addition to the specimens from the component materials. These latter results show that the composite yields at a value close to that of the lower strength backup material, but has a tensile strength between that of both components. This is what would be expected from a consideration of the relative contributions from the frontal and backup materials. The tensile strength of air melt Lot II appears to be low, probably because of the low ductility and fracture prior to maximum load.

Table II. TYPICAL MECHANICAL PROPERTIES OF DUAL HARDNESS STEEL

Dual Hardness Steel Armor		0.1% YS (ksi)	0.2% YS (ksi)	UTS (ksi)	Elon (%)	R.A. (%)	Hardness R_C
Ausformed[a]	Frontal	233	258	349	7	-	57
	Backup	200	220	289	9	-	50
Air Melt Lot I[a,b]	Frontal	-	219	361	6	15	61
	Backup	-	183	262	9	45	51
	Composite	-	185	319	9	12	-
Air Melt Lot II[b]	Composite	173	197	261	1	3	61[c] 50[d]
Vacuum Induction Melt	Composite	155	184	285	5	7	58[c] 48[d]

a. Ausformed and air melt lot I properties determined by producers
b. Air-melted material (lots I & II) supplied by two different producers
c. Frontal hardness
d. Backup hardness

Little information has been provided to date on either impact or fracture toughness of these materials. In-house programs are currently underway to study toughness and stress corrosion behavior of DHS.

The response of air melt Lot II DHS to cyclic loading is shown in Figure 1 for a minimum to maximum stress ratio of 0.1. In the as-received surface condition, short lives are encountered at maximum stresses in the vicinity of 100 ksi. When the maximum stress is lowered to approximately 70 ksi a life of at least 1×10^6 cycles can be expected. Orientation does not appear to markedly affect fatigue behavior. This probably is due to the cross-rolling techniques used during fabrication. However, surface condition is important. In the as-received condition, the surface contains many stress raisers which can serve as initiation sites for failure (see insert of Figure 1 showing scanning electron micrograph of initiation sites on the as-received surface). At maximum stress level of 80 ksi, improving the surface by grinding prior to testing markedly increases the life compared to the as-received condition as shown in Figure 1. It should be noted that grinding also removed a small amount of decarburization which probably reduced the fatigue life by lowering the surface strength level.

Typical fatigue crack growth rate data at several different maximum stresses are presented in Figure 2, for the ausformed steel. The cracks grow at an increasing rate as the number of cycles increases. In general, the cracks grow at a faster rate in the hard, frontal material, and lag behind in the softer backup material. On these 3-inch-wide specimens, the crack in the hard face typically will grow completely across the width of the specimen by fatigue, followed by fast fracture of the remaining backup material. As the gross stress level is increased, the number of cycles to failure decreases in customary fashion. Of particular interest in these DHS specimens is the observation that the lag in crack growth in the backup material increases as the maximum gross stress increases, e.g., at the onset of fast fracture in the backup, the fatigue crack length is smaller the higher the stress.[4]

For monolithic materials, crack growth data such as are shown in Figure 2 can be analyzed to produce data relating the crack growth rate and the stress intensity factor range ΔK. The growth rate per cycle da/dn is determined by the slope of curves, and ΔK is calculated from the instantaneous crack length "a" and the stress range $\Delta\sigma$, by the use of a formula of the form $\Delta K = k\sqrt{a}\,\Delta\sigma$, where k is a constant. For many materials, the results are found to obey an equation of the type frequently employed, $da/dn = C(\Delta K)^n$, where C is a constant, and the growth rate exponent n is in the range 2 to 4. This equation is useful in calculating crack growth rates and residual fatigue lives under various loading conditions.

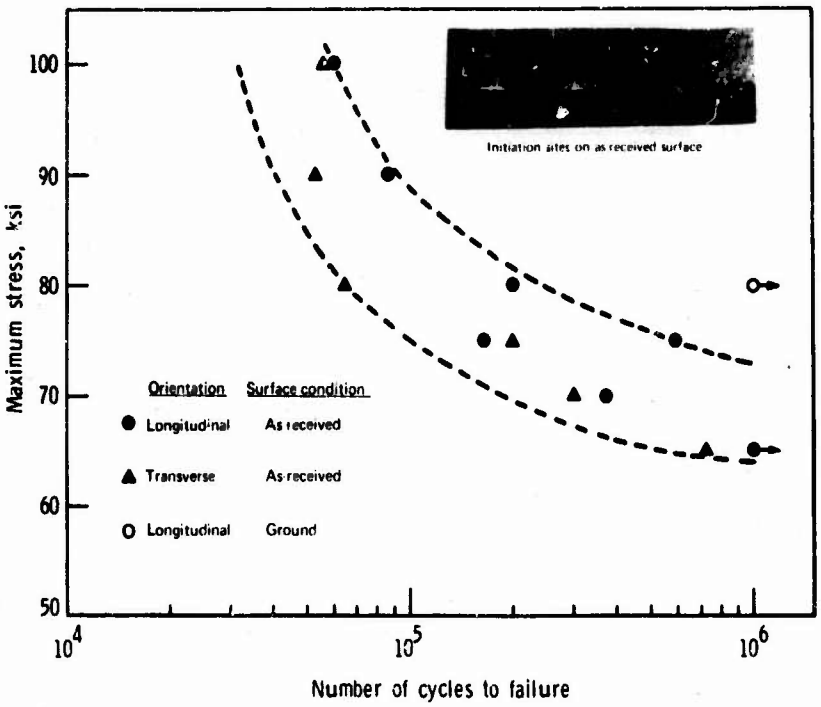

Figure 1. Maximum stress versus the number of cycles to failure fatigue curve for air-melted (lot II), heat-treatable, dual hardness steel. Minimum stress: Maximum stress ratio 0.1.

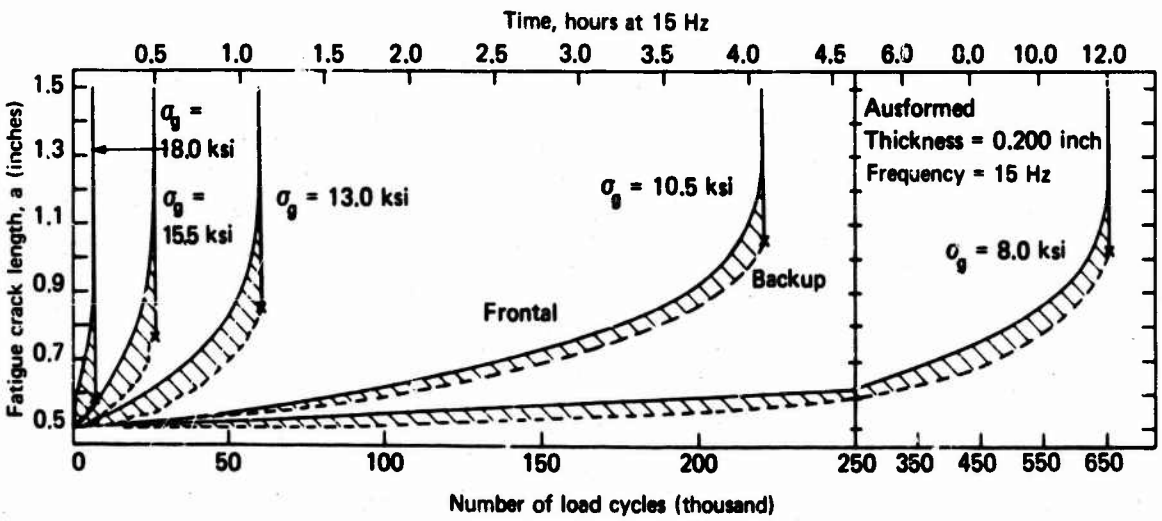

Figure 2. Fatigue crack length as a function of the number of load cycles and stress for ausformed, dual hardness steel

This procedure is not readily applicable to a layered composite such as DHS, however, since the crack length in one layer is influenced by the interface and the crack length in the other layer. Furthermore, since the crack front is not a straight line through the thickness, the stress intensity factor cannot easily be calculated. Nonetheless, based on the experimental observations of the faster growth rate in the frontal material and the increasing acceleration of the frontal growth with stress, it is possible to conclude that the relative growth rate of the frontal and backup materials must have the relationship shown schematically in Figure 3, and that the growth rate exponent "n" is higher for the frontal material. This is true for most, but not all the DHS types investigated, as will be noted later.

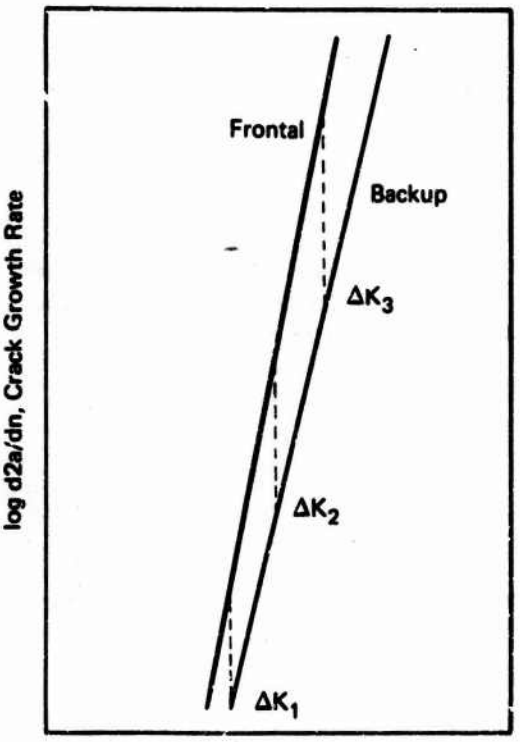

Figure 3. Schematic crack growth rates versus the stress intensity factor range for monolithic components of dual hardness steel

The frequency of loading can have an important effect on crack propagation. Crack growth curves for air melt Lot I at three different stress levels and frequencies 4 and 15 Hz are shown in Figure 4. These frequencies are typical of those that would be encountered by DHS in a helicopter, where the frequency of loading is determined by the product of the number of rotor blades and the revolutions per minute of the rotor. From Figure 4 it can be seen that at the lowest stress used, 8 ksi, there is little difference between the two frequencies, but at gross stress levels of 10.5 and 13 ksi the crack growth rates and the fatigue lives are markedly affected, with the lower frequency giving rise to the poorer properties.

Frequency effects can be caused by inherent effects of strain rate on the materials properties or by adiabatic heating. Neither of these factors are considered to be significant here. It is well known that the environment (air, water vapor, etc.) can have an accelerating influence on crack growth. For a given number of cycles, specimens tested at a lower frequency are exposed to the environment for a longer time, and hence suffer more degradation. It is believed that such environmental factors are active in DHS.

Another major variable influencing crack growth is the temperature. Figure 5 shows the effect of temperature variations from -60 F to +200 F on crack growth in the VIM steel. As the temperature decreases, the rate of crack growth decreases, and the fatigue life increases. The crack length at failure decreases, however. Note for this VIM steel that the rates of crack growth for the frontal and backup materials are quite similar, in contrast to the ausformed and air melt Lot I steels shown in Figures 3 and 4.

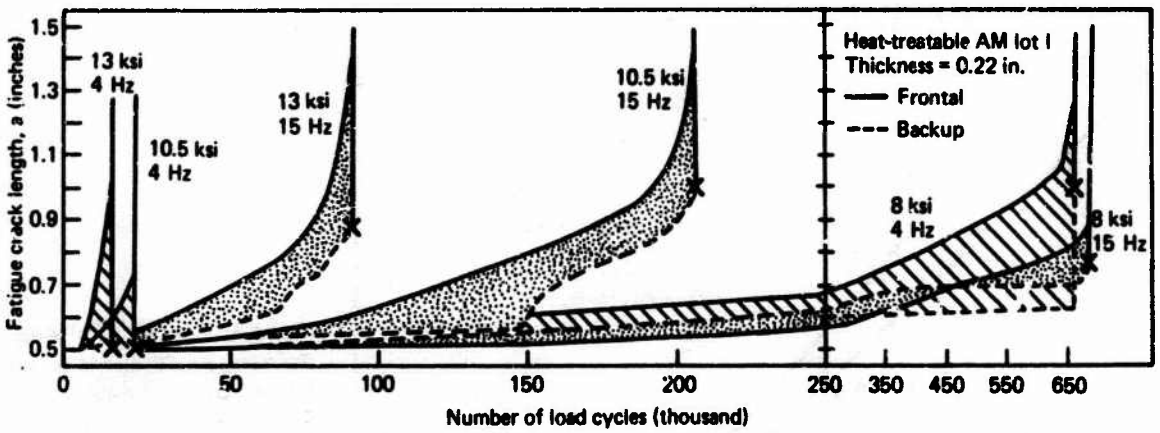

Figure 4. Fatigue crack length as a function of the number of load cycles and frequency for air-melted (lot I), heat-treatable, dual hardness steel

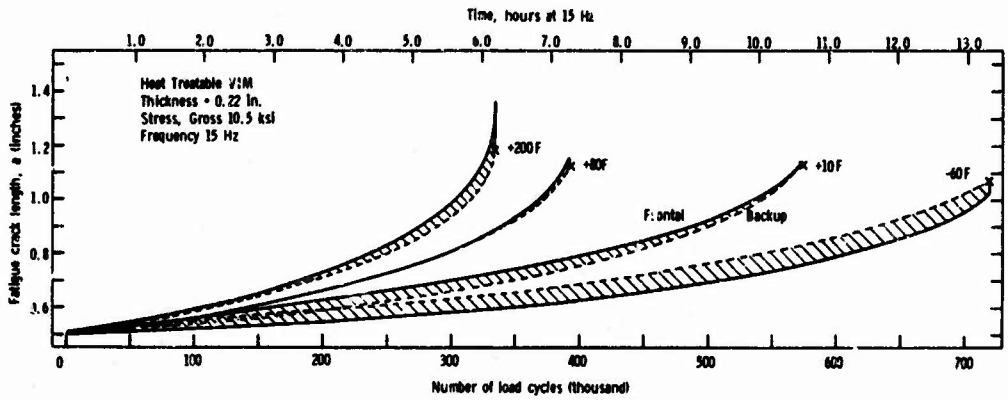

Figure 5. Fatigue crack length as a function of the number of load cycles and temperature for vacuum-induction-melted, dual hardness steel

A metallurgical variable of interest may be the direction of growth with respect to the rolling direction of the plate. For example, in the ausformed steel, the fatigue life of a precracked specimen at a gross stress of 10.5 ksi was 189,000 cycles when the crack propagated in the transverse direction, but only 140,000 cycles when the crack propagated in the longitudinal direction. At 13 ksi, the lives were 58,000 and 28,000 cycles. This difference in properties is related to banding and alignment of nonmetallic inclusions in the rolling direction during the rolling of the plate. This effect would be a maximum in a steel such as the ausformed steel, and would be much less in conventionally processed air-melted and vacuum-induction-melted steels, as was seen in Figure 1.

Based on the above observations, two comments can be made. These pertain to (1) the influence of metallurgical variables, and (2) residual life at anticipated service stress. It should be emphasized that the various dual hardness steels have varying chemistries and processing histories, and hence varying properties. Note that air melt Lot I and the VIM steels have similar compositions, although they have been tempered to different hardness levels. A comparison of the fatigue lives for notched specimens over a range of gross stresses is shown in Figure 6. The ausformed and air melt Lot I steels have the shortest lives, while the limited data for the VIM steel show it to have markedly superior fatigue properties.

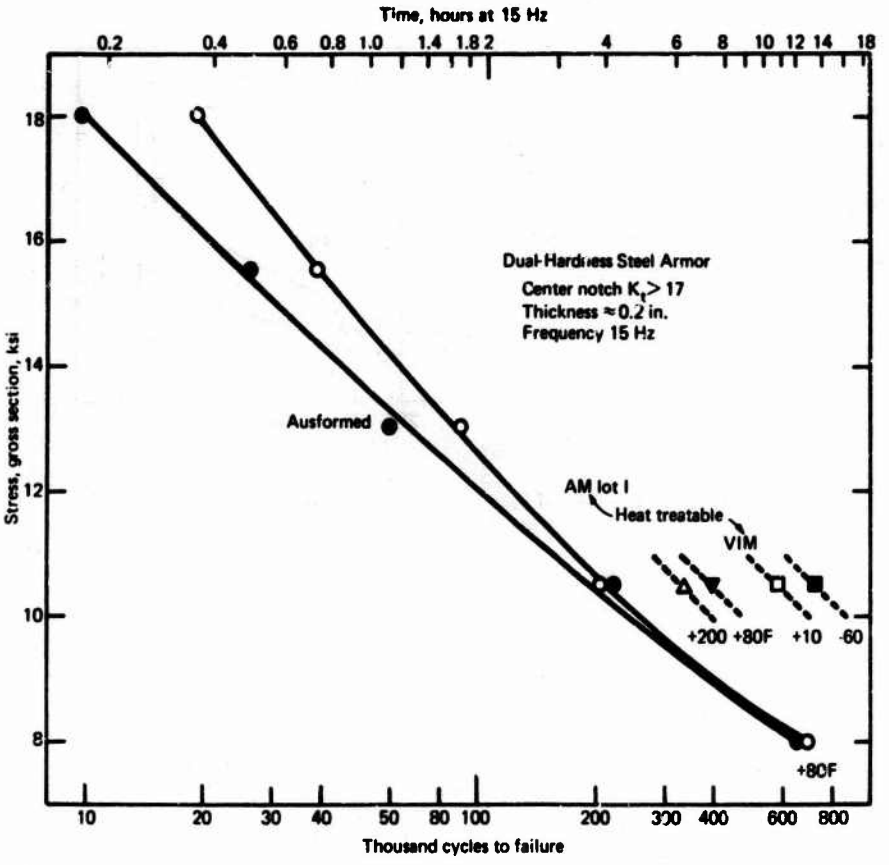

Figure 6. Gross section versus the number of cycles to failure for notched specimens of dual hardness steel. Specimens 3.0 in. wide with 1.0 in. center notch

Whether this difference is due to the vacuum melting or to the difference in hardness level is not known. Concerning expected service behavior, stress levels below 10 ksi are anticipated. At this stress level and at a frequency of 15 Hz, the residual life in the presence of a one-inch sharp crack (K_t > 17) will be greater than 4 hours for all materials investigated, as shown in Figure 6. Battle damage which provides similar stress intensity levels can be expected to provide correspondingly similar lives at the same stress levels. However, the importance of environments, residual stress levels resulting from joining and fabrication, and surface preparation should be considered. These areas are presently under investigation.

Ballistic Damage

Ballistically impacted steel armor can suffer a wide range of damage, depending on the type and size of projectile, velocity, obliquity, thickness of the armor plate, and properties of the armor.[7] This damage in turn will determine whether the component is destroyed or has sufficient residual strength or residual life to complete its assigned mission.[8,9] In this report, only impacts at 0 degrees obliquity are considered. At low hardness levels, penetration is accompanied by extensive plastic deformation, with a bending of the plate leading to tensile cracking or "petaling" on the rear surface. Another type of damage is "plugging" in which a projectile-sized plug is pushed out under thermoplastic or adiabatic shear conditions. This occurs at high hardness levels. The plate thickness to projectile diameter ratio influences the type of damage, with plugging favored by low ratios and petaling by high ratios. Another type of damage is front or back

spall, where high tensile stresses cause a chunk of the armor to fracture on a plane parallel to the surface and fly off. This type of fracture occurs more frequently under high velocity impact or where there is a plane of weakness in the armor, caused by banding or, in the case of DHS, by a poor interfacial bond. Delamination at the interface may be associated with the spall. Associated with these three types of fracture may be extensive radial cracking around the point of impact. The failure modes may not always be well described by these idealized mechanisms, or mixtures of the types may be encountered.

Some typical examples of ballistic damage encountered in DHS are shown in Figure 7. The first pair of photos (a) show plugging and radial cracking on the front face. The rear face probably petaled, but most of the deformed area spalled off, leaving some radial cracks. The second pair of photos (b) shows a partial penetration, with a probable front spall of the frontal material and petaling on the backup material, in the third pair of photos (c) is shown an example of plugging or conical spall, with some radial cracking in the front face. The fourth (d) and fifth (e) pair of photos show ballistic damage in the VIM steel by caliber 0.30 AP and ball ammunition. In both cases there is plugging, with cracks tending to form logarithmic spirals along planes of maximum shear stress in the plate. The rear surface shows evidence of plastic deformation and spalling of the backup material.

Applying a load during ballistic impact can increase the extent of radial cracking type of damage as can be seen in Figure 8. Here, test plates of air melt Lot II impacted with caliber 0.30 ball at a velocity sufficient to cause complete penetration show a marked increase in the extent of damage as the applied load is increased. The applied stress can be increased until the resultant damage is sufficient to cause fracture upon ballistic impact. This stress level, termed σ_f, was established at 26 ksi for the caliber 0.30 ball and 34 ksi for the AP. The effect of stress level on ballistic damage is shown in Figures 9 and 10 for the ball and AP projectiles. In terms of the number, maximum length, and accumulated length of ballistically induced cracks it is seen that the ball projectile is more damaging than the AP, which tended to produce plugging, thus accounting for the lower critical stress value. Note that in one instance (specimen 12, Figure 10), damage comparable to the ball projectile was obtained for the AP projectile. It is also interesting to note that the cracks described in Figures 9 and 10 did not penetrate through the thickness. No evidence of crack formation was found on the backup portion of any of the specimens in this series.

Damage under load was not confined to radial crack formation. There were isolated instances of frontal spall and debonding at the hard-soft layer interface, both occurring at the higher applied stress levels for both AP and ball ballistic impacts.

A marked improvement in ballistic performance was noted with the vacuum-induction-melted DHS. No fracture upon ballistic impact was noted at stress levels of 45 ksi for the ball and 50 ksi for the AP projectiles. Both of these stress levels exceed σ_f noted previously for heat-treatable air melt Lot II DHS. Such behavior is attributable to a lower propensity for crack formation during ballistic impact as shown in Figure 11.

Comparative measurements of ballistically induced cracks reveal that the greatest improvement in resistance of VIM material to ballistic damage occurred for plates impacted with caliber 0.30 ball projectile.

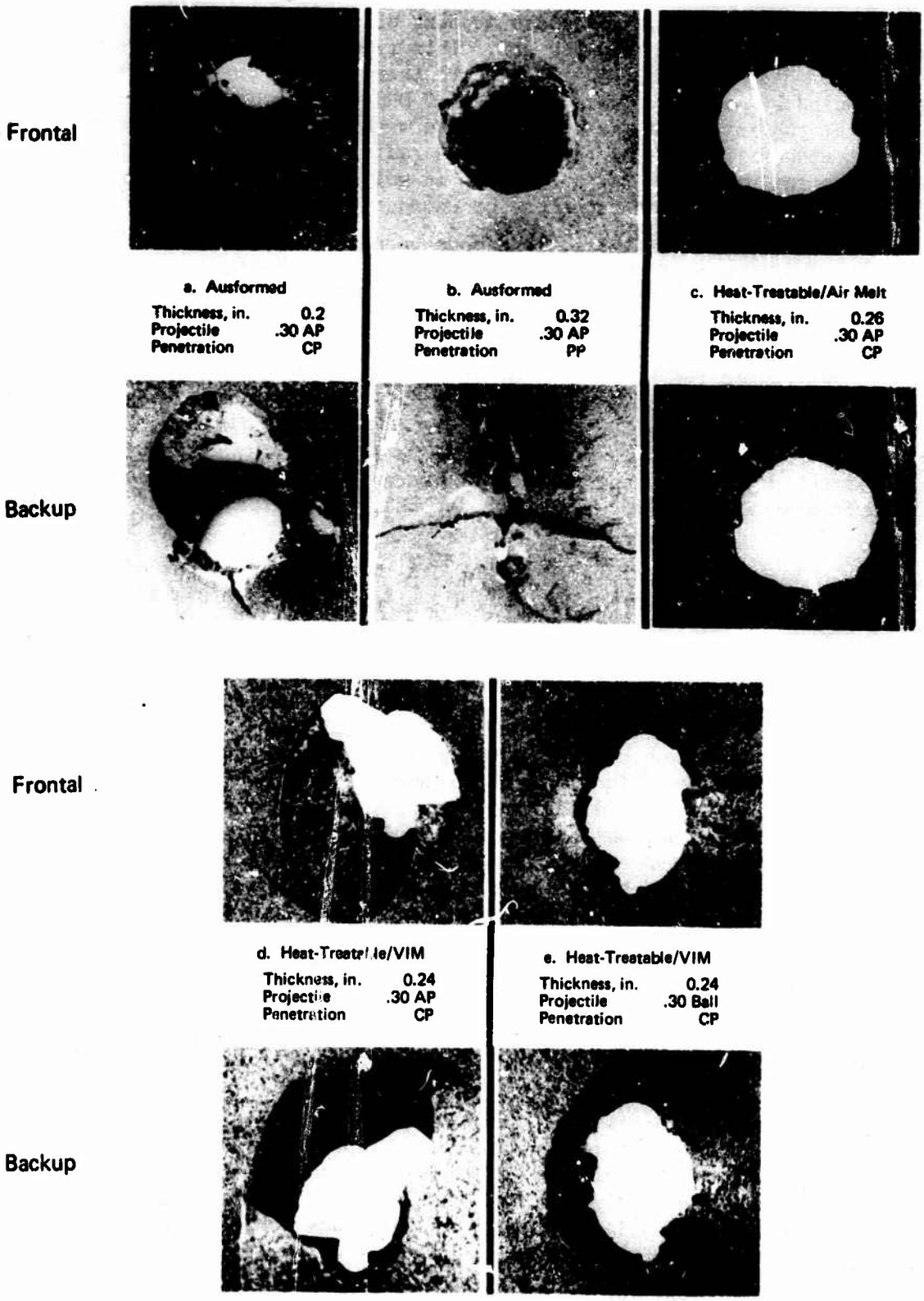

Figure 7. Typical ballistic damage patterns for ausformed and heat-treatable dual hardness steel

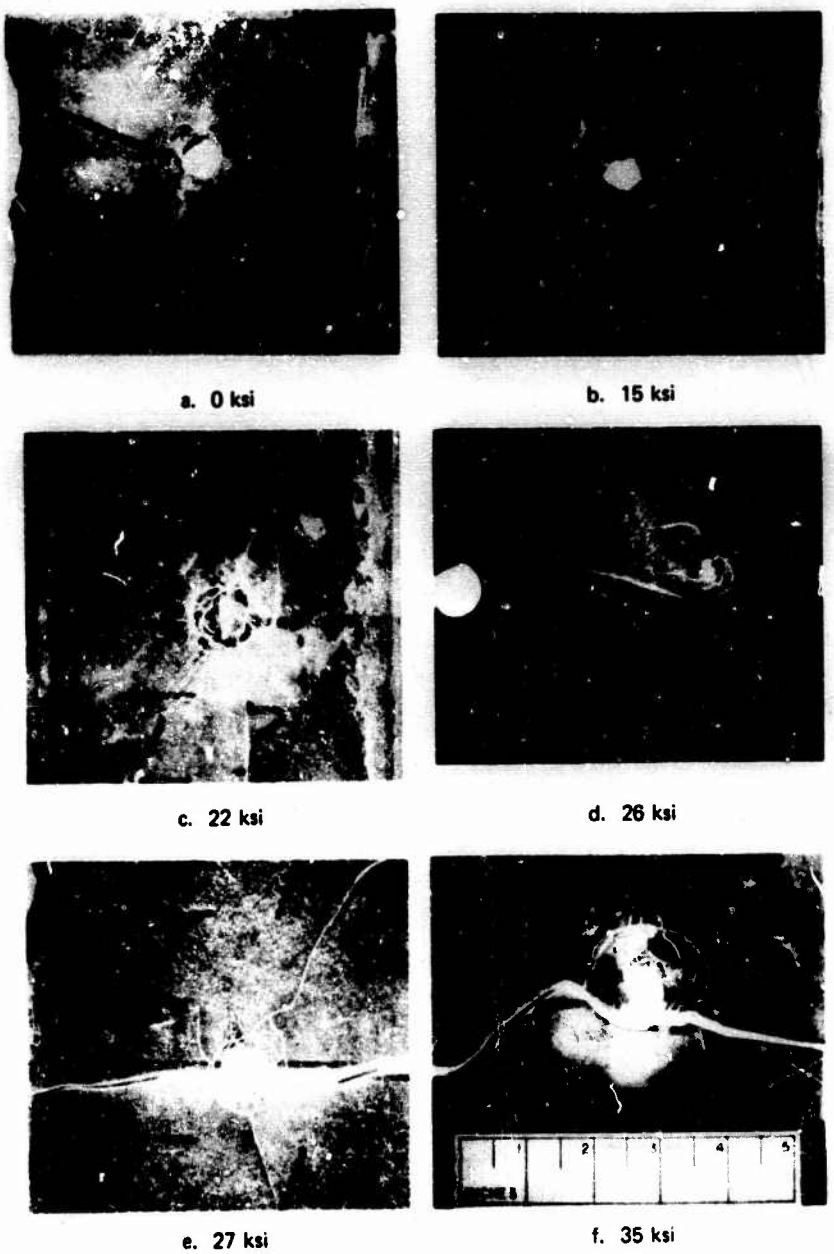

Figure 8. Ballistic damage resulting from impact of caliber 0.30 ball projectile at various applied stress levels. Material is air-melted (lot II), heat-treatable, dual hardness steel.

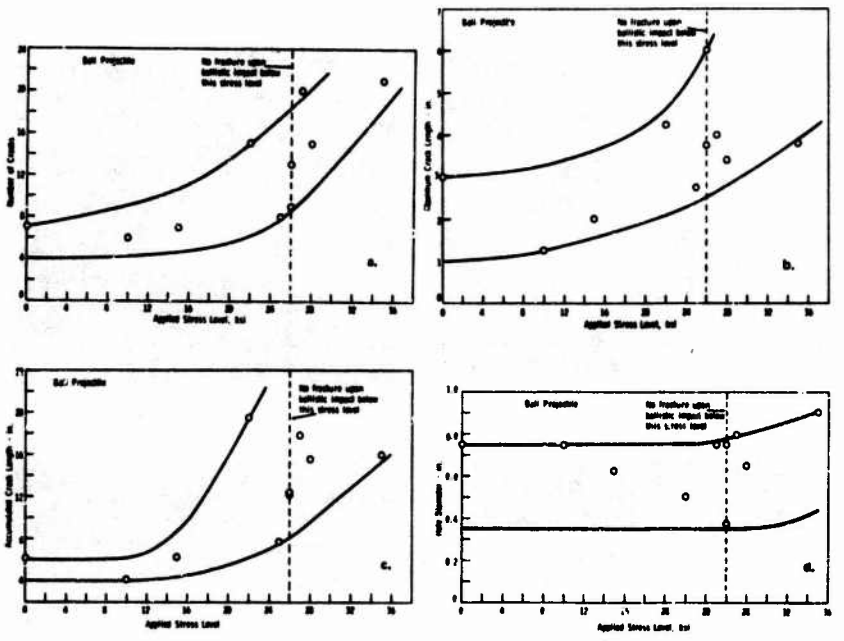

Figure 9. Effect of applied stress level on (a) number of cracks; (b) maximum crack length; (c) accumulated crack length and (d) hole diameter resulting from ballistic impact of caliber 0.30 ball projectile. Material is air-melted (lot II), heat-treatable, dual hardness steel.

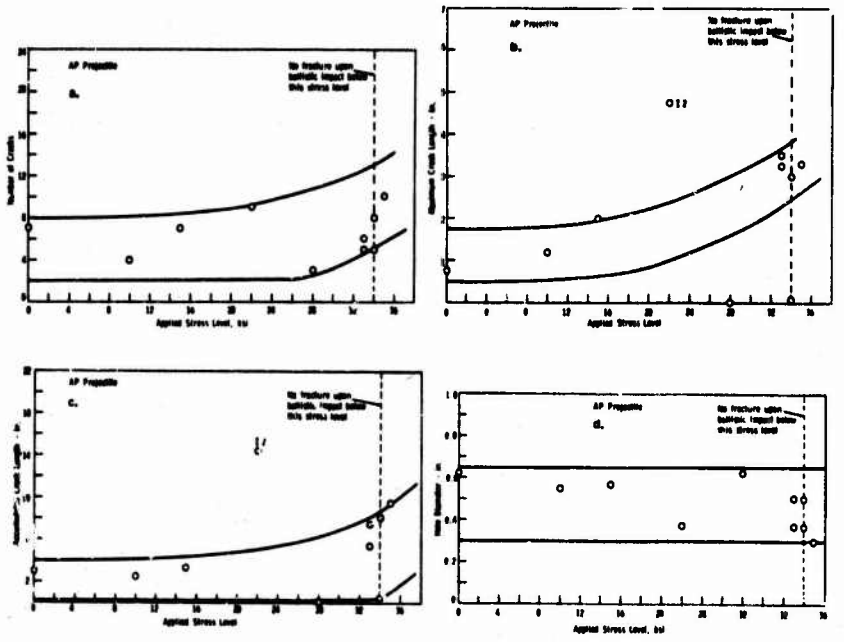

Figure 10. Effect of applied stress level on (a) number of cracks; (b) maximum crack length; (c) accumulated crack length and (d) hole diameter resulting from ballistic impact of caliber 0.30 AP projectile. Material is air-melted (lot II), heat-treatable, dual hardness steel.

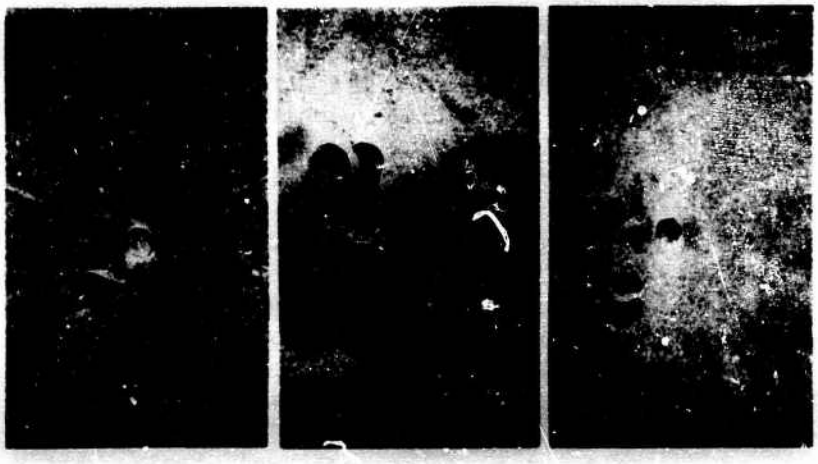

a. 45 ksi b. 27 ksi c. 10 ksi

Figure 11. Ballistic damage resulting from impact of caliber 0.30 ball projectile at various applied stress levels. Material is vacuum-induction-melted, heat-treatable, dual hardness steel.

Effect of Ballistic Damage on Residual Properties

Ballistic damage can cause considerable structural damage to a component, both by the removal of load-carrying cross section, and by the stress-concentrating effect of cracks or other notches formed during impact. The residual strength is influenced by the size of the damaged area, the radius of curvature at the crack tip, and the orientation of any cracks with respect to the major direction of loading. In this regard, a circular plugged hole would be less detrimental than radial cracking emanating from a plastically deformed petaled region. The strength of ballistically damaged structures using a fracture mechanics approach has been treated previously.[9]

Base-line tensile properties of the various types of dual hardness steel armor were shown in Table II. A complete penetration of the air melt Lot II armor lowers the residual strength to about one fourth of the undamaged strength level. There is further degradation in the residual strength of test plates ballistically impacted under load as shown in Figure 12. The drop to the 50 ksi residual strength level occurred for plates ballistically impacted near σ_f, the critical fracture stress. This is due to the increase in extent of cracking at these applied stress levels (Figure 9).

If failure of the component does not occur directly on impact, or by the application of a sudden load exceeding the notch strength, the residual life under fatigue conditions becomes especially important. The repeated application of a stress can cause either the initiation and growth of cracks in the impacted area, or the growth of cracks that formed during the projectile impact. When these cracks reach a critical size, the entire component may then fail.

Some results for five series of "fatigue" specimens cut from ballistically impacted plate are presented in Table III. In each series, up to five projectile velocities were used to determine a ballistic limit, encompassing a range from partial penetration (PP) to complete penetration (CP). The velocity increments and levels were arbitrary and are not the same within or between each series.

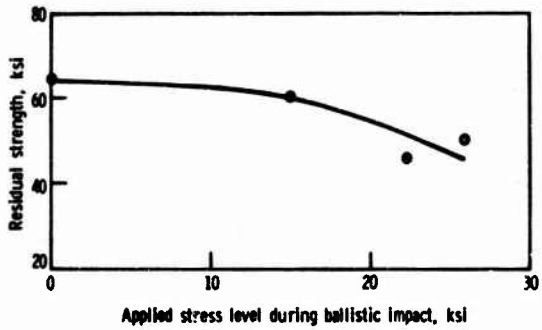

Figure 12. Effect of applied stress level during ballistic impact by caliber 0.30 ball projectile on residual strength. Material is air-melted (lot II), heat-treatable, dual hardness steel.

The differences in results between the different steels are striking. For two thicknesses of ausformed DHS, the residual fatigue life actually increases as the projectile velocity is increased and complete penetration occurs. For the heat-treatable air melt Lot I and the VIM steel the reverse is true, and the residual life decreases as projectile velocity increases. After giving allowance to the difference in stress range used during testing, a factor of 10 or 20 in life between 18 and 10.5 ksi (from Figure 6), the heat-treatable VIM steel is seen to have superior life to the air melt Lot I or the ausformed steel. This would indicate that based on an anticipated service stress level of 10 ksi as discussed earlier, the ballistically damaged VIM material would exhibit a life exceeding 10 hours.

These differences in behavior can be attributed not only to the inherent fatigue properties of each steel, but also to the damage caused during ballistic impact. Some of the fractured specimens listed in Table III were examined to determine the sequence of failure. Figures 13 to 15 show a photograph and sketches of three specimens. The ausformed steel hit at velocity level 3, Figure 13, showed extensive cracking around the point of impact on the hard face, although none of the cracks were perpendicular to the tensile axis. An extensive delaminated area occurred. Fatigue crack growth initiated in the frontal material and grew on both sides. Subsequently the crack grew into the backup material. Fast fracture occurred after 10,900 cycles when the crack had grown almost across the specimen. In the ausformed steels, low penetrator velocities caused delamination and plastic deformation of the backup material. Cracking was observed in the front and rear surfaces, especially with partial penetrations. At the higher velocities there was a tendency to form a large hole by spalling, with no long, unfavorably oriented cracks. The radial cracking and large delaminated area probably account for the poor residual life of this material.

Table III. RESIDUAL LIFE OF BALLISTICALLY DAMAGED DUAL HARDNESS STEEL

.30 AP Projectile Velocity Level	Cycles to Failure Fatigue Stress 3 to 18 ksi at 15 Hz		
	Ausformed		Heat-Treatable Lot 1
	t=0.2 in.	t=0.32 in.	t=0.26 in.
1	PP 6,100	PP 900	PP >>55,700
2	PP 6,100	PP 800	CP >>27,700
3	CP 10,900	PP 13,500	CP 44,100
4	CP 84,700	CP 41,000	CP 18,300
5	CP >>24,400	CP 20,400	CP 8,500

Proj. Velocity Level	Cycles to Failure Fatigue Stress 3 to 10.5 ksi at 15 Hz	
	Heat-Treatable VIM	
	.30 AP	.30 Ball
1	CP >3,880,000	PP >2,500,000
2	CP 975,060	PP 1,545,590
3	-	CP 930,370
4	-	CP 1,138,810
5	-	CP 765,460

PP, partial penetration from ballistic impact
CP, complete penetration from ballistic impact
>, fatigue test stopped
>>, premature failure due to pin holes

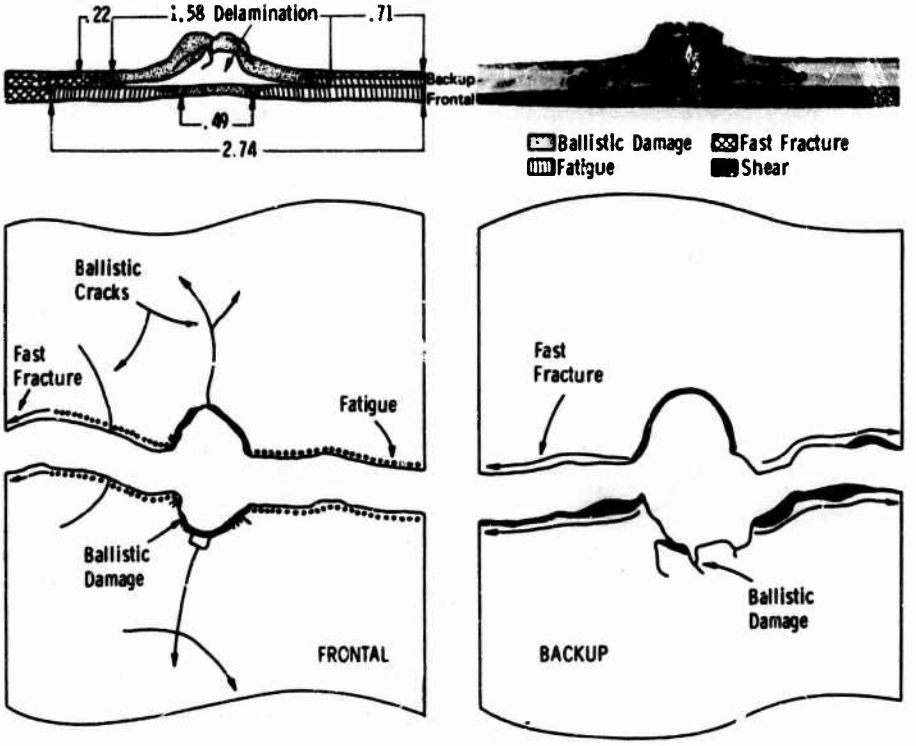

Figure 13. Ballistic damage, subsequent fatigue crack propagation and fast fracture for 0.2 in. ausformed dual hardness steel. Complete penetration with caliber .30 AP. Fatigue stress 3.0 to 18.0 ksi at 15 Hz. Cycles to failure 10.9 x 10^3.

In the air melt steel Lot I, a partial penetration provided very little damage. Figure 14 is typical of damage caused by complete penetration. There is little evidence of plastic deformation, but rather a conical plug, larger than the projectile diameter, has been pushed out. There may be some spalling associated with the plugging, but no delamination at the interface was noted. Radial cracking in this frontal material was observed, especially at higher velocities. Failure occurs by growth of cracks by fatigue from the damaged area across most of the width of the frontal materials and into the backup, followed by fast tensile fracture of the remaining cross section.

An entirely different behavior is exhibited by the heat-treatable VIM steel, Figure 15. This material showed extensive impact damage over a range of velocities. The cracking, in both front and rear faces, tended to follow logarithmic spirals. This was accompanied by plastic deformation of the backup material. Some spalling and delamination was noted. Fatigue cracks started at the cracks and grew across the frontal material and into the backup, followed by fast tensile fracture. The high residual life of this steel is connected with the nondamaging nature of the cracks (in contrast to radial cracks) and the inherently high crack growth resistance of the frontal and backup materials.

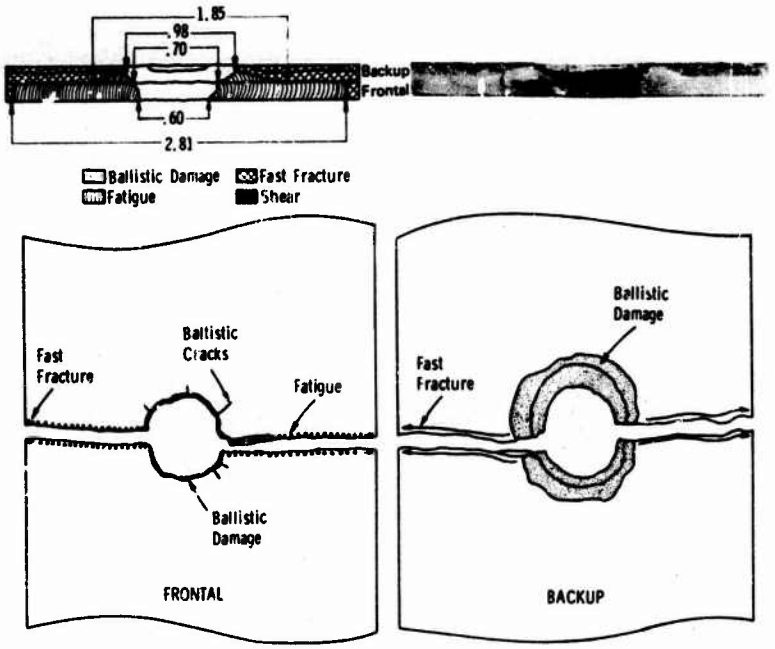

Figure 14. Ballistic damage, subsequent fatigue crack propagation and fast fracture for 0.26 in.-thick air-melted (lot I), heat-treatable dual hardness steel. Complete penetration with caliber 0.30 AP. Fatigue stress 3.0 to 18.0 ksi at 15 Hz. Cycles to failure 44.1 x 10^3.

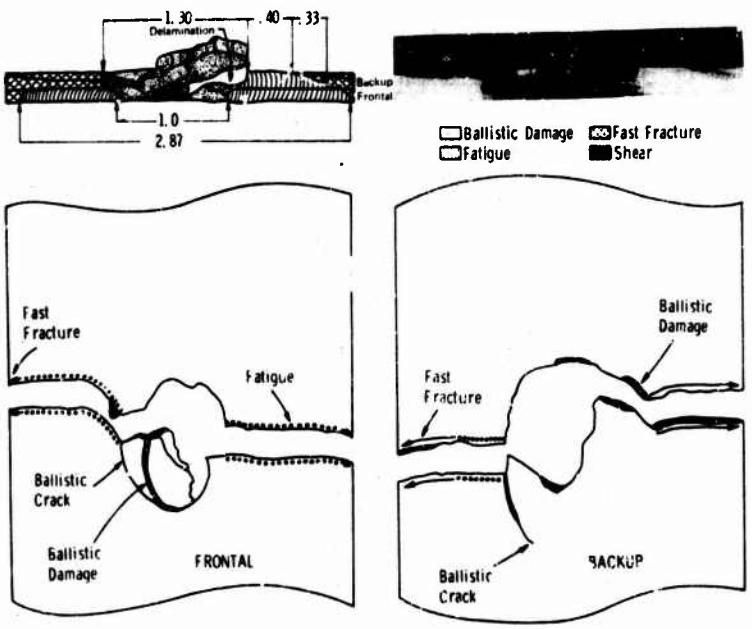

Figure 15. Ballistic damage, subsequent fatigue crack propagation and fast fracture for 0.24 in.-thick vacuum-induction-melted dual hardness steel. Complete penetration with caliber 0.30 AP. Fatigue stress 3.0 to 10.5 ksi at 15 Hz. Cycles to failure 9.75 x 10^5.

These results show that the residual strength and life of ballistically damaged DHS armor is determined in a complex way by the damage suffered by the armor during impact and the inherent mechanical properties of the two components of the armor.

SUMMARY AND CONCLUSIONS

Requirements for improved ballistic protection of helicopters have pointed to the use of dual hardness steel armor as a structural material. Four different lots of dual hardness steel with target hardness levels of R_c 60 for the frontal material and R_c 50 for the backup have been investigated. One lot had been produced by ausforming, the other three were conventional heat-treatable roll-bonded steels. Two of these lots were produced from air-melt steels, the third from vacuum-induction-melted steel.

The tensile and yield strengths of the steel were high, consistent with the high hardness. Tension-tension fatigue tests with as-processed surfaces showed a fatigue life in excess of 10^6 cycles at about 70 ksi. This could be improved by the removal of surface defects by grinding.

Crack growth tests under cyclic loading conditions were conducted for several of the lots. The crack growth rate increased with stress level. The cracks grow at a different rate in the frontal and backup material, with the growth rate generally higher in the hard frontal material. This difference in growth rate increasing stress level. The crack growth rate increases with decreasing frequency of loading, suggesting an influence of environment on the growth rate. Temperature is also an important variable, with the growth rate increasing with temperatures over the range -60 to +200 F. The fatigue life in the precracked condition was best for the vacuum-induction-melted steel. Fracture toughness data on these steels are needed.

Ballistic damage with caliber 0.30 ball and AP ammunition was studied. Typical types of damage included plastic deformation or petaling, thermoplastic shear or plugging, delamination, spalling, and front and rear cracking. The imposition of a tensile stress during ballistic impact led to increased amounts of ballistic damage by cracking, and above a critical stress value, failure of the entire plate. The type of damage varied markedly with the steel.

The residual strength decreased with increasing amounts of ballistic damage. Residual life in fatigue of ballistically damaged panels was found not to be a function of projectile velocity. Rather the life was found to depend on the extent and type of damage during impact as well as the inherent mechanical properties of the armor. For the VIM material, it was shown that based on anticipated service stress level of no more than 10 ksi, the ballistically damaged material would exhibit a residual fatigue life exceeding 10 hours.

ACKNOWLEDGMENT

The authors would like to thank Mr. Ronald A. Swanson for his contributions to this work.

LITERATURE CITED

1. BURR, C. W., DEGNAN, W. G., GRUMM, A. W., and McCAUL, C. O. *Aerial Armored Fuselage Engineering and Manufacturing Report, Part I (U).* Sikorsky Aircraft Division, Contract DAAG 46-69-C-0159, AMMRC CR 70-2/1, 1970.

2. GREENWOOD, J. D., and HILL, R. M. *Manufacturing Technology Using Dual-Hardness, Heat-Treatable Steel Armor.* FMC Corporation, Contract DAAG 46-68-C-0074, AMMRC CR 69-09, 1969.

3. HICKEY, C. F. *Mechanical Properties and Bonding Efficiency of Steel Composites.* Army Materials and Mechanics Research Center, AMMRC TR 67-12, 1967.

4. ANCTIL, A. A., and KULA, E. B. *Fatigue Crack Propagation in Armor Steels.* Army Materials and Mechanics Research Center, AMMRC TR 69-25, 1969.

5. SWANSON, R. A., and ANCTIL, A. A. *Dual-Hardness Steel Armor - Observations on Material Characteristics and Specimen Preparation.* Army Materials and Mechanics Research Center, AMMRC TN 71-2, 1971.

6. CHAIT, R., and CURTL, C. H. *Ballistic and Mechanical Properties of Dual Hardness Steel Armor (U).* (Confidential Report), Army Materials and Mechanics Research Center, AMMRC SP 72-8, 1972.

7. BREYER, N. N. *Armor and its Application to Vehicles (U).* Ordnance Engineering Design Handbook, (Confidential), ORDP 20-170, 1961.

8. MURPHY, T. M. *Aerial Armored Fuselage Materials Evaluation (U).* Sikorsky Aircraft Division, Contract DAAG 46-71-C-0042, Final Report, AMMRC CR 71-11, August 1971, Confidential Report.

9. JENSEN, J. E. *The Ballistic Damage Characteristics and Damage Tolerance of Wing Structural Elements.* Damage Tolerance in Aircraft, ASTM-STP 486, 1971, p. 215-229.